[CANCER RESEARCH 63, 5446–5453, September 1, 2003]

# Autotaxin Hydrolyzes Sphingosylphosphorylcholine to Produce the Regulator of Migration, Sphingosine-1-Phosphate

**Timothy Clair,[1] Junken Aoki,[2] Eunjin Koh, Russell W. Bandle, Suk Woo Nam, Malgorzata M. Ptaszynska, Gordon B. Mills, Elliott Schiffmann, Lance A. Liotta, and Mary L. Stracke**

*Laboratory of Pathology, National Cancer Institute, NIH, Bethesda, Maryland 20892 [T. C., E. K., R. W. B., S. W. N., M. M. P., E. S., L. A. L., M. L. S.]; Graduate School of Pharmaceutical Sciences, the University of Tokyo, Tokyo 113, Japan [J. A.]; and Department of Molecular Therapeutics, M.D. Anderson Cancer Center, Houston, Texas 77030 [G. B. M.]*

## ABSTRACT

**Autotaxin (ATX) is an exoenzyme that potently induces tumor cell motility, and enhances experimental metastasis and angiogenesis. ATX was shown recently to be identical to serum lysophospholipase D activity, producing lysophosphatidic acid (LPA) from lyso-glycerophospholipids. LPA, itself a strong chemoattractant for tumor cells, may mediate the actions of ATX. We now extend the substrate specificity to sphingosylphosphorylcholine (SPC), which ATX hydrolyzes to sphingosine-1-phosphate (S1P). Under migration assay conditions, this novel reaction for the production of S1P has a substrate (SPC) $K_m = 0.23 \pm 0.07$ mM. In our responder cell lines (NIH3T3 clone7 and A2058), S1P exerts maximal biological effects at concentrations of 10–100 nM and is mimicked in its biological effects by ATX plus SPC. These effects include inhibition of ATX- and LPA-stimulated motility, and elevation of activated Rho. In NIH3T3 clone7 cells stimulated with platelet-derived growth factor and treated with 10–25 nM S1P, motility is not inhibited and activation of Rho is unaffected, indicating that S1P possesses specificity in its effects. The exoenzyme ATX can potentially regulate diverse processes such as motility and angiogenesis via the S1P family of receptors. Because ATX hydrolyzes nucleotides, lyso-glycerophospholipids, and phosphosphingolipids into bioactive products, it possesses the ability, depending on the availability of substrates, to act as positive or negative regulator of receptor-mediated activity in the cellular microenvironment.**

## INTRODUCTION

ATX,[3] a $M_r$ 125,000 glycoprotein, is a member of the nucleotide pyrophosphatase/PDE family of ecto/exoenzymes (1), originally defined by their ability to hydrolyze phosphoester bonds in nucleotides *in vitro* (2, 3). ATX is a multifunctional protein, stimulating motility at subnanomolar concentrations (1), enhancing the invasive, tumorigenic, and metastatic potentials of *atx*-transfected *ras*-transformed NIH3T3 cells (4), and inducing an angiogenic response in Matrigel plug assays (5). In addition, ATX mRNA expression has been associated with BMP2-mediated osteogenic and chondrogenic differentiation in mice (6), and has been found in oligodendrocytes and choroid plexus of developing rats during the time of active myelination (7). Therefore, ATX acts on both tumor and normal cells, contributing to an invasive or aggressive phenotype in tumor cells.

A possible explanation for the multiple biological activities associated with ATX was provided recently when ATX was found to possess lyso-PLD activity, hydrolyzing LPC to produce the bioactive phospholipid, LPA. Two separate groups isolated lyso-PLD activity from FCS (8) and from human plasma (9), and found the resulting protein to be identical to ATX. Aoki *et al.* (10) have since shown that ATX has the capacity to hydrolyze several other glycerophospholipids to produce LPA, including lysophosphatidylserine, lysophosphatidylethanolamine, and lysophosphatidylinositol. Their data indicated a substrate preference for lysophospholipids, because phosphatidylcholine was a weak substrate compared with LPC.

LPA is both a mitogen and a motogen that acts through G protein-associated *Edg* receptors (Edg-2/$LPA_1$, Edg-4/$LPA_2$, Edg-7/$LPA_3$). LPA has been associated with tumor aggressiveness, stimulating invasion of a mesothelial cell monolayer by either rat hepatoma or human small cell lung carcinoma cell lines (11). LPA also plays a role in angiogenesis by stabilizing endothelial monolayer barriers (12). Because LPA has been shown to stimulate VEGF expression by ovarian cancer cells, LPA could act as a mediator for tumor cell-directed angiogenesis (13). These data suggest that many of the known properties of ATX could be explained by its capacity to hydrolyze membrane or secreted glycerophospholipids to produce the bioactive effector, LPA.

In the present manuscript, we show that the substrate specificity of ATX/lyso-LPD extends to the phosphosphingolipid, SPC, which it hydrolyzes to produce S1P. Although S1P has been shown to stimulate endothelial cell motility and tube formation, it inhibits motility in several tumor and leukocyte cell lines (14). Using A2058 and NIH3T3 (clone7) cells as models, we found that S1P inhibits the migration responses to both ATX and LPA; but in NIH3T3 cells, S1P has no effect on PDGF-induced migration. Like LPA, S1P acts through G protein-associated Edg receptors (Edg-1/$S1P_1$, Edg-5/$S1P_2$, Edg-3/$S1P_3$, Edg-6/$S1P_4$, Edg-8/$S1P_5$). We examine Edg receptor expression in A2058 and NIH3T3 clone7 cells, and demonstrate that S1P activates the small GTPase Rho in both cell lines.

## MATERIALS AND METHODS

**Reagents.** LPA (18:1) and S1P were from Biomol Research Laboratories, Inc. (Plymouth Meeting, PA). LPC (18:1), SPC, and phosphatase inhibitor mixtures I and II were from Sigma-Aldrich Corp. (St. Louis, MO). PTX and protease inhibitor mixture I were from Calbiochem (San Diego, CA). Agarose pull-down resin for GTP-bound Rho and MLB were from Upstate (Waltham, MA). PDGF was purchased from Biosource International (Camarilla, CA).

**Cell Lines.** A2058 (15), the green monkey kidney cell line (COS-1), and NIH3T3 clone7 cells were maintained in DMEM supplemented by 2 mM glutamine, 1× penicillin/streptomycin, and 10% (v/v) heat-inactivated fetal bovine serum. The NIH3T3 clone7 cell line was kindly provided by Dr. Douglas Lowy (NIH, Bethesda, MD).

**ATX Preparations.** myc-ATX, cloned from a rat liver library, was prepared as described previously (8). vATX, cloned from an MDA-MB-435 cell library, was prepared from a Vaccinia viral lysate, as described previously, through the conA-agarose step (16). Homogeneously purified hisATX was

Received 2/26/03; revised 5/1/03; accepted 5/28/03.

The costs of publication of this article were defrayed in part by the payment of page charges. This article must therefore be hereby marked *advertisement* in accordance with 18 U.S.C. Section 1734 solely to indicate this fact.

[1] To whom requests for reprints should be addressed, at Laboratory of Pathology, National Cancer Institute, NIH, Building 10, Room 2A33, 9000 Rockville Pike, Bethesda, MD 20892. Phone: (301) 496-1843; Fax: (301) 402-8911; E-mail: timclair@helix.nih.gov.

[2] Present address: Microarray and Expression Genomics Section, Department of Pathology, College of Medicine, The Catholic University of Korea, Seoul, 137-701 Korea.

[3] The abbreviations used are: ATX, autotaxin; DMEM-BSA, DMEM supplemented with 1 mg/ml BSA; Edg, endothelial differentiation gene; hisATX, His-tagged recombinant human ATX, purified to homogeneity; LPA, lysophosphatidic acid; LPC, lysophosphatidylcholine; lyso-PLD, lysophospholipase D; MLB, magnesium lysis buffer; myc-ATX, myc epitope ATX cloned from a rat liver library; PDE, phosphodiesterase; PDGF, platelet-derived growth factor; PTX, pertussis toxin; RT-PCR, reverse transcription-PCR; S1P, sphingosine-1-phosphate; SPC, sphingosylphosphorylcholine; vATX, recombinant human ATX prepared from viral lysate; HRP, horseradish peroxidase; ERK, extracellular signal-regulated kinase.

isolated from conditioned medium of a selected clone of High Five cells, described below.

**Isolation and Purification of Stably Transfected High Five Cells Secreting hisATX.** Using the plasmid vector pMIB/V5-His (Invitrogen Life Technologies, Inc., Carlsbad, CA), an ATX fusion protein was created by replacing the 31 $NH_2$-terminal amino acids of ATX (intracellular and transmembrane domains) with honeybee melittin secretion signal, and adding a V5 epitope and 6XHis tag to the COOH terminus. ATX cDNA was prepared by PCR using recombinant human ATX cloned into the eukaryotic expression vector pcDNA3.1 (Invitrogen Life Technologies, Inc.) as described previously as template (17). ATX cDNA was digested with appropriate restriction enzymes and ligated into identically cleaved vector. DH5$\alpha$ cells were transformed with the constructed vector and selected with 100 $\mu$g/ml ampicillin, as recommended by the manufacturer. This amplified ATX-containing vector was then transfected into High Five cells using lipofectin. The transfected High Five cells were grown in Ultimate Insect serum-free medium, supplemented with 50 $\mu$g/ml blasticidin to allow selection of a stable cell line, then maintained in Ultimate Insect serum-free medium supplemented with 10 $\mu$g/ml blasticidin. Conditioned medium from ATX-secreting High Five cells was concentrated using an Amicon ultrafiltration device ($M_r$ 30,000 molecular weight cutoff), precipitated with 60% saturated ammonium sulfate, and subjected to conA-agarose and to nickel-agarose chromatography (Novagen, Madison, WI), including 20% ethylene glycol in all of the buffers. The highly purified hisATX was then dialyzed to remove imidazole.

**Preparation of ATX Mutant Proteins.** Plasmids containing wild-type or mutant ATX cDNA were transfected into COS-1 cells, and the resultant medium was harvested, concentrated, and partially purified with conA-agarose (18).

**Lyso-PLD Assay.** For the experiment shown in Fig. 1*B*, recombinant ATX (vATX or hisATX) was incubated with 1 mM LPC (from egg) or SPC in the presence of 100 mM Tris-HCl (pH 9.0), 500 mM NaCl, 5 mM $MgCl_2$, and 0.05% Triton X-100 for 1 h at 37°C. The liberated choline was detected by an enzymatic photometric method using choline oxidase (Asahi Chemical, Tokyo, Japan), HRP (Toyobo, Osaka, Japan), and TOOS reagent [*N*-ethyl-*N*-(2-hydroxy-3-sulfopropyl]-m-toluidine (Dojin, Tokyo, Japan) as a hydrogen donor (19, 20).

For Fig. 1*D* (5 $\mu$l samples with 50 $\mu$l reaction volume) and for Fig. 1*E* (20 $\mu$l samples with 100 $\mu$l reaction volume), samples were diluted in DMEM-BSA and incubated at 37°C in the presence of the indicated concentrations of either LPC or SPC. DMEM-BSA was used to mimic the conditions of the motility assays. Released choline was detected by a modification of the enzymatic photometric assay described above. A 950 $\mu$l mixture containing 50 mM Tris-HCl (pH 8.0), 5 mM $CaCl_2$, 0.3 mM *N*-ethyl-*N*-(2-hydroxy-3-sulfopropyl)-m-toluidine (TOOS), 0.5 mM 4-aminoantipyrene, 5.3 units/ml HRP,

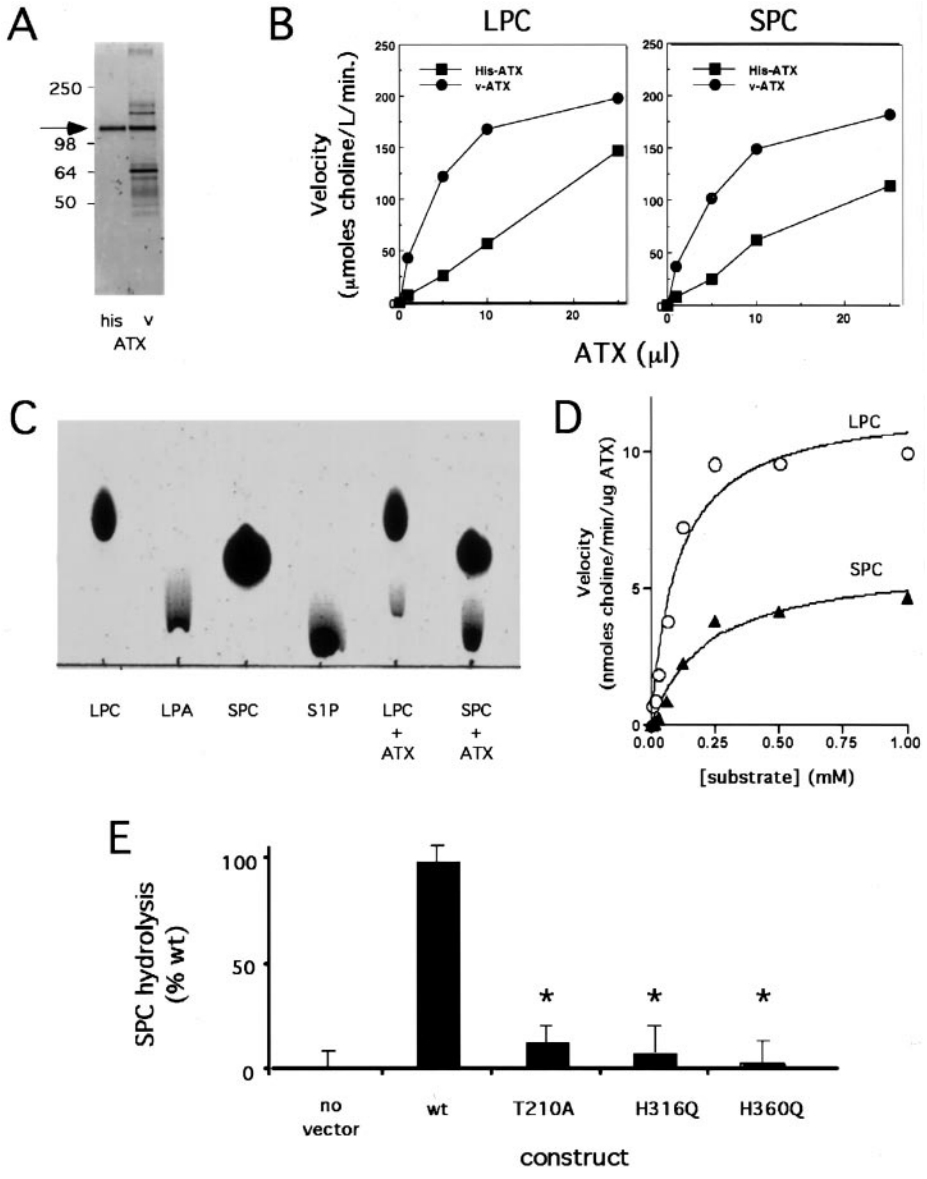


Fig. 1. Enzymatic properties of ATX hydrolysis of SPC. *A*, silver staining of electrophoretically resolved preparations (8–16% acrylamide Novex minigels); *his*, hisATX; *v*, vATX; *arrow* indicates ATX. *B*, choline release assay ("Materials and Methods") using the enzyme preparations, hisATX and vATX, as indicated, and the substrates LPC and SPC, as indicated above the panels. *C*, TLC and iodine vapor detection of phospholipids after incubation of myc-ATX with LPC or SPC. *D*, reaction rate *versus* substrate concentration curves for LPC and SPC with reactions carried out in DMEM-BSA. *E*, choline release assays comparing wild-type (*wt*) to mutant ATXs. Values, expressed as % wt, are mean; *bars*, ± SE; *, $P < 0.001$ compared with wt. Means were compared using ANOVA/Tukey's post-test (GraphPad Prism, San Diego, CA).

and 2 units/ml choline oxidase (all reagents from Sigma) was added to the reaction mixture and incubated for an additional 15 min at 37°C. Absorbance was read at 555 nm and converted to nmol of choline by comparison to a choline standard curve. For the experiment shown in Fig. 1*E*, conA-agarose-purified conditioned media from transfected COS cells were adjusted to equal ATX protein concentrations based on intensity of immunoblot signals.

**Lipid Analysis.** For TLC analysis the enzyme reaction was performed as described above (see lyso-PLD Assay) except that 0.1% BSA (fatty acid-free; Sigma) was added instead of 0.05% Triton X-100. Phospholipids in reaction mixtures were extracted (21) under acidic conditions by adjusting the pH to 3.0 with 1 N HCl to recover LPA efficiently. Lipids in the aqueous phase were re-extracted and pooled with the previous organic phase. The extracted lipids were dried, dissolved in chloroform:methanol (1:1) and used for TLC analysis using chloroform:methanol:formic acid:$H_2O$ (60:30:7:3; v/v). Phospholipids were detected using iodine vapor. The recovery of lipids was monitored by the addition of trace amounts of 1-[$^3$H]oleoyl-LPC or 1-[$^3$H]oleoyl-LPA to the samples. Under the described conditions, recoveries of 1-[ $^3$H]oleoyl-LPC and 1-[$^3$H]oleoyl-LPA were always >95%.

**Analysis of Signaling Proteins.** Three million NIH3T3 cells or 6 million A2058 cells were seeded in complete medium on 100-mm diameter gelatin-coated dishes (0.01% gelatin and 0.1% acetic acid; 37°C, 1 h, 10 ml PBS). After overnight culture the medium was removed and, after a PBS wash, replaced by DMEM-BSA. After an overnight incubation in serum-free conditions the volume of medium was adjusted to 2 ml, and treatments were initiated. Medium was aspirated; cells were washed twice with 5 ml PBS and lysed with 1 ml MLB with the addition of 1× protease inhibitor mixture I, and 1× phosphatase inhibitor mixtures I and II. After 3 min, lysate was harvested by scraping and centrifugation (14K rpm; 20 s).

Activated Rho was detected by pull-down isolations using agarose resins (10 $\mu$g) attached to glutathione *S*-transferase-linked interaction domains from rhotekin, the direct downstream effector of Rho. The resin was mixed with 450 $\mu$l of lysate and incubated in microtubes at 4°C for 2 h. GTP-bound Rho was recovered by centrifuging (14K rpm; 20 s) and washing (600 $\mu$l three times) of the resin with MLB. Rho was released from the final pellet by adding 35 $\mu$l SDS gel sample buffer (Novex) and heating at 95°C for 10 min, followed by centrifugation (14K rpm at 20°C; 1 min). Thirty-$\mu$l samples from pull-down isolations (GTP-Rho) or (17 $\mu$l) cell lysate added to equal volume of 2× sample buffer (total Rho) were subjected to electrophoresis (Invitrogen Life Technologies, Inc.; 14% acrylamide, 1.5 mm thickness minigels; 125 V, 1.75 h) and electroblotting (Invitrolon membranes; 0.45 $\mu$m pores; Invitrogen Life Technologies, Inc.) in Tris-glycine transfer buffer. Unoccupied protein binding sites on blotted membranes were blocked by incubation with 75 mg/ml glycine, 1 $\mu$l/ml Tween 20, and 50 mg/ml nonfat dry milk in water at room temperature for 2 h. Total and activated Rho were detected by incubating the membranes with anti-Rho A mouse monoclonal antibody (1:200; Santa Cruz Biotechnology, Inc., Santa Cruz, CA) for 2 h at room temperature. Membranes were washed three times (5 min) in 20 ml of wash buffer [50 mM Tris-HCl (pH 7.4), 1 mg/ml BSA, and 1 $\mu$l/ml Tween 20] and incubated with HRP-conjugated goat-antimouse IgG (1:5000; Pierce, Rockford, IL) for 1 h at room temperature. After additionally washing the membranes (20 ml wash buffer; 3 × 5 min), signals were developed using enhanced chemiluminescence.

For analysis of total or phosphorylated forms of Akt or ERK, separate 50-$\mu$l aliquots of the lysate were added to equal volumes of 2× sample buffer and heated at 95°C for 5 min. Samples (17 $\mu$l) were subjected to electrophoresis and electroblotting as described above. The phosphorylated forms of Akt and ERK were detected by incubating the blotted membranes (room temperature; 2 h) with a mixture of two antibodies in wash buffer that included 50 mg/ml dry milk. Anti-P-Akt (1:400) and anti-P-ERK (1:1,500), as well as anti-T-Akt (1:400) and anti-T-ERK (1:400) were rabbit polyclonal antibodies (Cell Signaling Technologies, Beverly, MA). These prepared membranes were then treated as detailed for Rho detection using HRP-conjugated goat-antirabbit IgG as secondary antibody (1:25,000; Pierce).

***In Vitro* Motility Assay.** Chemotaxis was assayed as described previously (22) and quantified by cell counting under light microscopy or by densitometric scanning and image analysis of the fixed and stained cells (Personal Densitometer SI and ImageQuant software; Molecular Dynamics).

**Detection of Edg Receptor mRNA Expression.** A2058 or NIH3T3 cells were grown to 80% confluency in Falcon 60-mm dishes, then total cellular RNA was isolated with TRIzol reagent per the manufacturer's instructions (Invitrogen Life Technologies, Inc.). Isolated RNA was suspended in 10 mM Tris with 1 mM EDTA. Complementary primers (Table 1) were used to amplify Edg receptor cDNA in 500-ng samples of total RNA, following the manufacturer's protocol with the Titan One Tube RT-PCR system (Roche Diagnostics Corporation, Indianapolis, IN). Positive controls used total human or mouse RNA from Biochain Institute, Inc. (Hayward, CA). Negative controls eliminated the reverse transcriptase step. The resulting cDNA products were separated on a 1.5% agarose gel, stained with ethidium bromide, and visualized under UV light.

Table 1 *Paired primers for amplification of human or mouse Edg receptor cDNA*

| Primer sequence | Primer name | RT-PCR product size (bp) |
|---|---|---|
| 5′ ggaagggagtatgtttgtggc 3′ | Edg1S | 778 |
| 5′ tgacgtttccagaagacata 3′ | Edg1A | |
| 5′ tttcacagccccagttca 3′ | Edg2S | 688 |
| 5′ cattctcatagtcctctggcga 3′ | Edg2A | |
| 5′ agggagggcagtatgttcg 3′ | Edg3S | 466 |
| 5′ gccacatcaatgaggaagaggat 3′ | Edg3A | |
| 5′ tggcctacctcttcctcatgttcc 3′ | Edg4S | 628 |
| 5′ attgaccagtgagttggcct 3′ | Edg4A | |
| 5′ agtggccattgccaaggtcaag 3′ | Edg5S | 425 |
| 5′ tagtgggctttgtagagga 3′ | Edg5A | |
| 5′ atcacgctgagtgacctgctca 3′ | Edg6S | 672 |
| 5′ tgcggaaggagtagatga 3′ | Edg6A | |
| 5′ cacatgtcaatcatgaggat 3′ | Edg7S | 493 |
| 5′ atggggttcacgacggagtt 3′ | Edg7A | |
| 5′ ctactgtcggggccgctcac 3′ | Edg8S | 658 |
| 5′ cggttggtgaacgtgtagatga 3′ | Edg8A | |
| 5′ catgtttgagaccttcaacac 3′ | $\beta$-actinS[a] | 716 |
| 5′ ctgcttgctgatccacatct 3′ | $\beta$-actinA[a] | |

[a] Positive control.

**Detection of Edg Receptor Protein Expression in A2058 Cells.** For detection of Edg-3/$S1P_3$ and Edg-5/$S1P_2$ proteins, subconfluent cells were grown in 150-mm diameter plates, washed twice with ice-cold PBS, then lysed (3 min) in ice-cold lysis buffer (10 mM HEPES, 1 mM EDTA, 250 mM sucrose, 1× protease inhibitor mixture I, and 1× phosphatase inhibitor mixtures I and II). Cells were scraped and transferred to a microtube. This lysate was passed through a 20-gauge needle, vortexed, then centrifuged (1,000 × *g*) for 10 min at 4°C to remove nuclei. The resulting supernatant was vortexed and centrifuged (3,000 × *g*) at 4°C for 10 min to reduce mitochondrial contamination. Semipurified supernatant protein concentrations were determined with Pierce MicroBCA kit, and then 20 $\mu$g of lysate were combined with SDS sample buffer, boiled, and subjected to electrophoresis (Invitrogen Life Technologies, Inc.; 18% acrylamide, 1.5 mm thickness minigels; 160 V; 7 h). Separated proteins were electroblotted to an Invitrolon membrane and blocked overnight at 4°C in the same blocking buffer as described above (in "Analysis of Signaling Proteins"). Membranes were washed three times (PBS, 1 mg/ml BSA, and 1 $\mu$l/ml Tween 20), then incubated for 2 h at room temperature in anti-Edg-3 or anti-Edg-5 (Antibody Solutions, Palo Alto, CA), both diluted 1:2,000 in wash buffer. Membranes were then washed six times (5 min) in the same buffer, incubated with HRP-conjugated goat-antimouse (1:10,000) for 1 h at room temperature, then washed again six times (5 min) and developed using enhanced chemiluminescence.

## RESULTS

**ATX Catalyzes the Hydrolysis of a Phosphosphingolipid Substrate.** After the discovery that LPC is efficiently hydrolyzed by recombinant ATX (8), we used a choline release assay to test the ability of independent preparations of ATX to catalyze hydrolysis of LPC as well as the alternative phospholipid substrate, SPC. Electrophoresis and sensitive silver staining of these ATX preparations revealed a single protein band (for hisATX) or a predominant band (for vATX) at the expected positions (Fig. 1*A*). These preparations were indistinguishable in 5′-nucleotide PDE activity, PTX-sensitive stimulation of migration, and immunoblot analysis, indicating that these preparations represent authentic ATX (data not shown).

The results of the choline release assay (Fig. 1*B*) demonstrate that ATX has activity toward the glycerophospholipid LPC as reported

previously (8) and show, for the first time, similar activity toward the phosphosphingolipid SPC. When normalized for ATX concentration, the specific activity of vATX was indistinguishable from the hisATX. To confirm these results, we used TLC analysis of the enzymatic products resulting from incubation of myc-ATX with LPC or SPC. The results, shown in Fig. 1*C*, indicate that ATX catalyzed the production of LPA from LPC and of S1P from SPC. Just as phosphatidylcholine had been shown to be a weak substrate compared with LPC (10), we failed to detect hydrolysis of sphingomyelin in our choline release assay (data not shown), indicating a selective substrate requirement for deacylation at the C2 position of the glycerol or sphingosine backbone.

Next, the hydrolytic activities of hisATX toward LPC and SPC were compared using the choline release assay, with reaction conditions similar to the migration assay (DMEM-BSA). For either substrate, the hydrolysis proceeded at a constant rate for at least 2 h. The enzymatic parameters $K_m$ and $V_{max}$ were determined for each substrate (Fig. 1*D*). The results for LPC ($K_m$ = 0.10 ± 0.03 mM; $V_{max}$ = 11.8 ± 0.9 nmol/min/$\mu$g) are in general agreement with previous reports (8, 9). The results for SPC hydrolysis ($K_m$ = 0.23 ± 0.07 mM; $V_{max}$ = 6.1 ± 0.7 nmol/min/$\mu$g) were comparable. The catalytic efficiency ($V_{max}/K_m$) for SPC was of the same order of magnitude, although somewhat (4.5-fold) lower compared with LPC.

The T210A mutant ATX protein has been reported to be deficient in phosphodiesterase activity and in its capacity to stimulate motility (23). We compared partially purified T210A ATX to the wild-type protein to determine its lyso-PLD (choline release) activity toward SPC (Fig. 1*E*). Just as it failed to stimulate phosphodiesterase activity, T210A failed to hydrolyze SPC. In addition, recently reported (18) nucleotide- and LPC-hydrolysis-deficient mutant ATXs (H316Q and H360Q) are also deficient in SPC hydrolysis (Fig. 1*E*). These data suggest that SPC hydrolysis by ATX has structural requirements in common with hydrolysis of nucleotides and LPC.

**The Enzymatic Product of SPC Hydrolysis by ATX Has Biological Activity.** Because the hydrolytic activity of ATX toward glycerophospholipids extended to phosphosphingolipids, it appeared that ATX might produce alternative, biologically and physiologically different, enzymatic products depending on the nature of the available substrate. To address this possibility we used the migration response of NIH3T3 and A2058 cells to hisATX or LPA.

Preliminary chemotaxis assays (data not shown) were performed with LPA, S1P, and SPC to establish effective concentration ranges for each. A2058 cells have a bipolar migration response to LPA that is maximal at concentrations of 0.250–5 $\mu$M, whereas the NIH3T3 migration response to LPA formed a plateau at concentrations from 0.250–20 $\mu$M. Of note, the $EC_{50}$ for ATX-stimulated migration is 300–500 pM (1). S1P (20–100 nM) inhibits maximal ATX- or LPA-stimulated migration responses in both cell lines to levels below basal migration. Within this same concentration range, S1P alone significantly inhibited basal migration of both lines, indicating that basal migration might be caused by an endogenous S1P-sensitive chemoattractant or by low levels of S1P-sensitive, cytokine-independent receptor activities. Similarly, SPC (50 nM to 10 $\mu$M) inhibited ATX-stimulated migration of both NIH3T3 and A2058 cells; however, at 1–10 $\mu$M, SPC alone also significantly inhibited background migration of both cell lines without affecting LPA-stimulated motility. A likely explanation for this observation is that SPC has low-affinity cross-reactivity with S1P receptors, as has been found in other systems (24, 25).

Representative data for these experiments are shown (Fig. 2*A*) for A2058 (Fig. 2, black bars) and for NIH3T3 (Fig. 2, gray bars) cells, comparing the effect of S1P (100 nM), SPC (100 nM), or a combination of SPC and ATX, on migration responses to ATX (3 nM) or LPA (1 $\mu$M). As noted, ATX-stimulated migration was inhibited in the presence of either S1P or SPC (for both cell types). LPA-stimulated migration was inhibited in the presence of S1P but not SPC. However, the combination of ATX and SPC significantly inhibited the LPA response of both cell types

These data strongly imply that inhibition of migration in the presence of SPC requires the ATX-catalyzed production of S1P. To test this hypothesis, we utilized the LPA-stimulated migration response in both cell lines (Fig. 2*B*). ATX or heat-inactivated ATX was added to 100 nM SPC and preincubated at 37°C for 3 h, then tested for inhibition of LPA-stimulated migration either directly or after heat inactivation of the ATX. For both cell lines, LPA-stimulated migration was inhibited by the heat-stable activity produced by incubation of active ATX and SPC. In contrast, incubation of heat-inactivated ATX with SPC failed to produce an inhibitor of migration.

To definitively assign inhibitor production to ATX, and to additionally confirm that enzymatic activity of ATX is required for the production of the heat-stable inhibitor, we tested 5′-nucleotide PDE-deficient mutant ATXs (T210A, H316Q, and H360Q; Ref. 18) for their ability to produce an inhibitor of LPA-stimulated migration. Wild-type or mutant ATX was incubated with 100 nM SPC at 37°C for 5 h to facilitate enzymatic activity, followed by an additional incubation at 95°C for 15 min to eliminate residual ATX activity. These prepared mixtures were tested for their effect on LPA-stimulated migration of A2058 cells (Fig. 2*C*). The same mutant ATX proteins that had failed to release choline from SPC (Fig. 1*E*) also failed to produce a heat-stable inhibitor of LPA-stimulated migration (Fig. 2*C*).

These data suggest that the production of the potent lysophospholipid mediators, LPA and S1P, may be regulated by the expression of ATX and the local availability of precursors. This is the first demonstration of inhibition of migration by an enzymatic product of ATX catalysis.

**S1P or (SPC + ATX) Strongly Enhances the Accumulation of GTP-Rho.** To address the possibility that the inhibition of migration by S1P might arise from nonspecific effects, we sought to evaluate the receptor-mediated nature of the effects of S1P, as well as SPC plus ATX, by detecting changes in signal transduction responses. hisATX, purified to homogeneity, was used for all of these experiments. ATX-stimulated migration responses of both NIH3T3 (data not shown) and A2058 cells (26) are sensitive to pretreatment of the cells with PTX (500 ng/ml). Initial signaling studies in our laboratory using serum-starved NIH3T3 cells showed that 7-min treatments with ATX, in the absence of exogenous substrate, resulted in the PTX-sensitive accumulation of activated (phospho-) forms of both Akt and ERK (Fig. 3*A*) as well as the PTX-insensitive accumulation of the activated (GTP-bound) form of the cytoskeletal regulator Rho (Fig. 3*B*).

In contrast, PDGF (5 ng/ml) is a strong PTX-insensitive chemoattractant for NIH3T3 cells (data not shown). PDGF treatment resulted in activation of Erk that was slightly higher than that seen with ATX treatment (163%), but activation of Akt was >8-fold higher with PDGF treatment. Both PDGF-stimulated responses were resistant to PTX, confirming that the PTX sensitivities of the ATX responses are specific to G protein-coupled signaling and not the result of nonspecific inhibition of the signaling network.

Because S1P has been shown to activate Rho (14), we took advantage of the NIH3T3 cell-signaling model to test the effect of S1P, or a combination of ATX and SPC, on the level of GTP-Rho. We stimulated serum-starved NIH3T3 cells with ATX (3 nM) in the presence or absence of SPC (50 nM) or S1P (5 nM), using SPC or S1P alone as controls, and monitored the activation state of Rho (Fig. 3*C*). Treatment (7 min) of NIH3T3 cells with ATX resulted in an increase in GTP-Rho above basal levels. In this experiment, SPC alone ap-

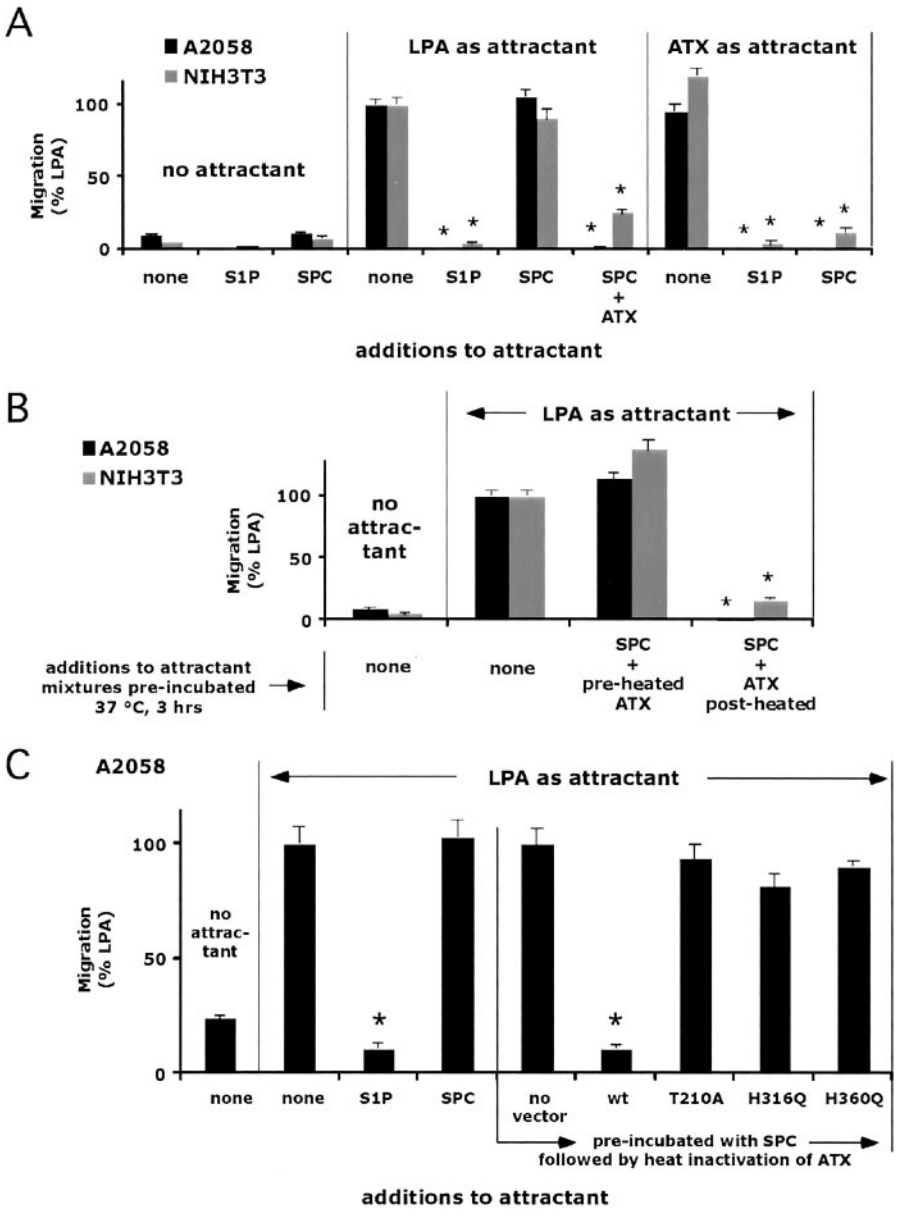


Fig. 2. ATX catalyzes production of bioactive phospholipids. Attractant mixtures were tested for chemotactic activity using A2058 (■) and NIH 3T3 (▨) cells. *A*, migration responses were measured to 3 nM ATX or 1 $\mu$M LPA in the presence of 100 nM S1P or 100 nM SPC. When LPA was the attractant, an additional condition was to add both 3 nM ATX and 100 nM SPC to the lower well. *B*, mixtures of ATX or heat-inactivated ATX were preincubated for 3 h with 100 nM SPC, as indicated, then tested directly or after a secondary incubation at 70°C (to inactivate the ATX) for their effect on LPA-stimulated migration. *C*, wild-type (*wt*) and mutant ATXs were preincubated for 5 h with 100 nM SPC, heat-inactivated, and compared for their ability to inhibit LPA-stimulated migration. S1P and SPC served as controls. Values, expressed as % LPA response, are mean; *bars*, ±SE; ∗, $P < 0.001$ compared with no addition (for *A* and *B*), or to no vector (for *C*). Means were compared as in Fig. 1.

peared to decrease GTP-Rho levels slightly in NIH3T3 cells, although in three experiments this varied from a slight decrease (two of three) to no effect (one of three; data not shown). This variation in low-level signals could easily arise from variation in GTP-Rho pull-down recovery and is unlikely to be significant. Treatment with S1P, or a combination of ATX plus either SPC or S1P, resulted in an increase in GTP-Rho that was greater than the level attained by ATX treatment alone (2.4–4-fold increase compared with ATX alone). Our data are consistent with the hypothesis that ATX catalyzes production of S1P from SPC because the combination of ATX and SPC mimicked the effects of S1P on activation of Rho. In this same experiment, PDGF treatment of NIH3T3 cells resulted in a decreased level of GTP-Rho compared with unstimulated cells (Fig. 3*C*, PDGF compared with none). As noted above, differences in low-level signals may not be significant. However, the effect of S1P in the presence or absence of PDGF (Fig. 3*C*, S1P compared with PDGF + S1P) indicates that PDGF inhibits the S1P-induced activation of Rho. We next directly compared the effect of S1P on the migration response of NIH3T3 cells to ATX or PDGF (Fig. 3*D*). The inclusion of S1P (10 nM) completely blocks the migration response to ATX but has no significant effect on the response to PDGF. It should be noted that higher concentrations of S1P (50–100 nM) caused a slight inhibition of PDGF-stimulated motility (data not shown). These data suggest that the inhibition of ATX-stimulated migration by S1P is relatively specific and does not arise from a general dysregulation of locomotion, that there is a correlation between high levels of GTP-Rho and the inhibition of migration, and that the resistance of the PDGF migration response to S1P treatment may be at least partially explained by the ability of PDGF to prevent the accumulation of GTP-Rho.

We tested the effect of PTX treatment on the activation of Rho by S1P or by the combination of SPC and ATX. The results, shown in Fig. 3*E*, indicate that the activation of Rho by either treatment was resistant to inhibition by PTX.

The effects of S1P (or SPC + ATX) treatment of A2058 cells (Fig. 3*F*) were identical to its effects on NIH3T3 cells, confirming the correlation between high levels of GTP-Rho and inhibition of motility. As with NIH3T3 cells, ATX treatment resulted in a moderate increase in GTP-Rho. SPC had no effect in two of three experiments but resulted in a slight increase above basal levels of GTP-Rho in the third (data not shown). S1P treatment resulted in a larger increase in

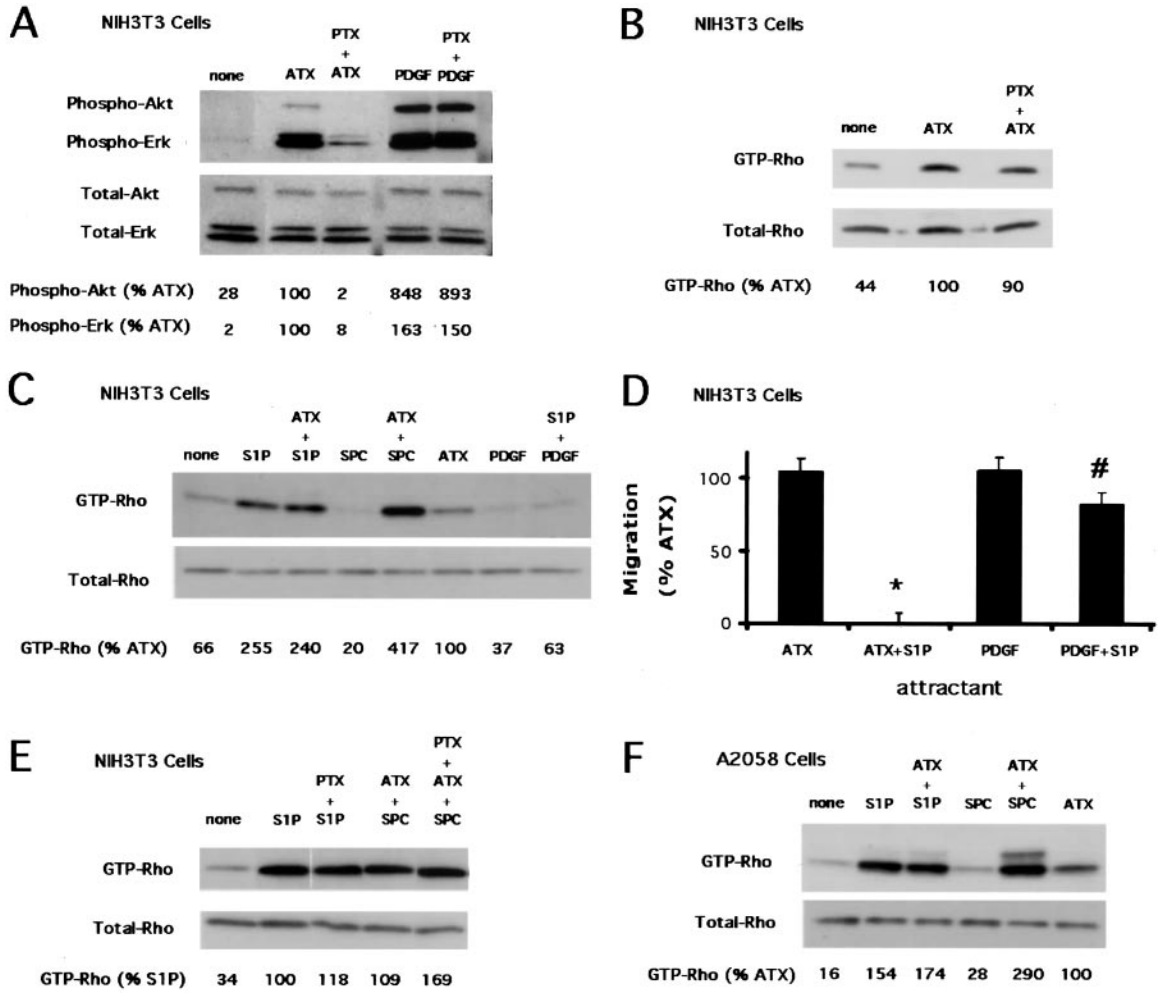


Fig. 3. S1P affects cell signaling in NIH3T3 clone7 stimulated by ATX but not by PDGF. Serum-starved cells (NIH3T3 clone7 in *A–C* and *E*; A2058 in *F*) were treated (8 min) without or with 3 nM ATX or 5 ng/ml PDGF, in the presence or absence of S1P or SPC (concentrations indicated), followed by immunoblot analysis of cell lysates ("Materials and Methods"). In some cases (*A*, *B*, and *E*), cells were pretreated for 2 h with 500 ng/ml PTX or with appropriate vehicle. *A*, autoradiograms compare the PTX sensitivities of Akt and Erk signaling responses to ATX and PDGF (treatments indicated *above the panels*). *B*, autoradiogram reveals the PTX insensitivity of ATX-induced Rho signaling. *C*, autoradiograms compare the effects of 5 nM S1P and 50 nM SPC on the activation state of Rho in the absence and presence of ATX or PDGF. *D*, the migration responses of NIH3T3 cells to 3 nM ATX or 5 ng/ml PDGF were tested in the absence and presence of 10 nM S1P. Values, expressed as % ATX response, are mean; *bars*, ±SE of stimulation above background; *, $P < 0.001$ compared with ATX; #, $P > 0.05$ compared with PDGF. Means were compared as in Fig. 1. *E*, PTX insensitivity of the Rho response is demonstrated for 10 nM S1P or for 50 nM SPC plus ATX. *F*, autoradiograms show the effect of 5 nM S1P or 50 nM SPC on Rho activation in A2058 cells in the absence or presence of 3 nM ATX. Autoradiograms were analyzed by densitometry; levels of the GTP-bound forms were normalized for total expression and shown as %ATX or %S1P, as indicated.

GTP-Rho than ATX alone, an effect mimicked by the combination of ATX and SPC.

**Edg Receptor Expression in A2058 and NIH3T3 Cells.** Using RT-PCR analysis we determined the Edg receptor (27) expression profile for the cell lines used in this study (Fig. 4*A*). Among the Edg family LPA receptors, A2058 and NIH3T3 clone7 cells both express Edg-2/$LPA_1$, Edg-4/$LPA_2$, and Edg-7/$LPA_3$. Both cell types show a positive migration response to LPA (Fig. 2*A*). Among the S1P receptors in this family, NIH3T3 and A2058 cells express both Edg-5/$S1P_2$ and Edg-3/$S1P_3$. Within the limits of RT-PCR analysis, neither of these cell lines expresses detectable Edg-1/$S1P_1$, Edg-6/$S1P_4$, or Edg-8/$S1P_5$. The Edg-5/$S1P_2$ receptor has been associated with inhibition of motility (28). Both Edg-1/$S1P_1$ and Edg-3/$S1P_3$ have been associated with PTX-sensitive migration responses to S1P (14).

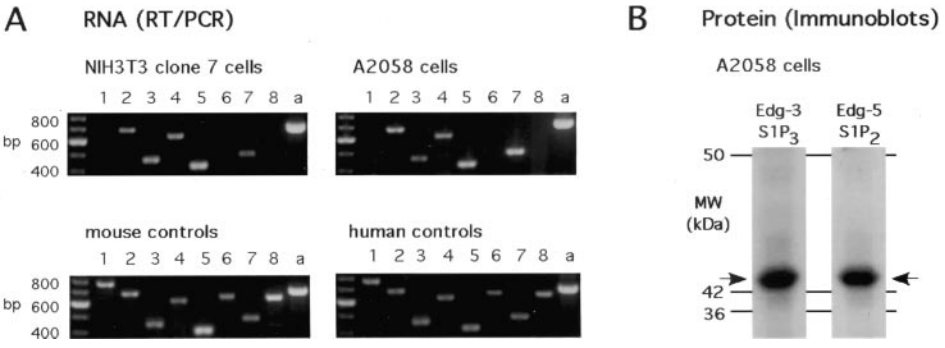


Fig. 4. Edg receptor expression in NIH3T3 clone7 and A2058 cells. *A*, mRNA expression in A2058 and NIH3T3 cells. Using specific primers that recognize both mouse and human Edg receptor cDNA (Table 1), Edg receptor expression was analyzed by RT-PCR. The Edg numbers (*above the gels*) are equivalent to: Edg-1/$S1P_1$, Edg-2/$LPA_1$, Edg-3/$S1P_3$, Edg-4/$LPA_2$, Edg-5/$S1P_2$, Edg-6/$S1P_4$, Edg-7/$LPA_3$, and Edg-8/$S1P_5$. *B*, protein expression in A2058 cells. Using primary antibodies specific for human/rat Edg-3/$S1P_3$ and Edg-5/$S1P_2$ in immunoblot analyses ("Materials and Methods"), both receptors were demonstrated in membrane preparations (20 $\mu$g total protein loaded in each well).

Using human/rat-specific antibodies for immunoblot analysis, we confirmed that both proteins, Edg-5/$S1P_2$ and Edg-3/$S1P_3$, are expressed in the A2058 cell line (Fig. 2*B*). Equivalent antibodies are not yet available for mouse Edg proteins.

## DISCUSSION

In this study for the first time we have shown that the substrate specificity for the exoenzyme ATX/lyso-LPD extends to the phosphosphingolipid, SPC, with the resultant product being the bioactive mediator, S1P. The catalytic efficiency for SPC hydrolysis to S1P is 4.5-fold lower than for hydrolysis of LPC to LPA; however, S1P exerts maximal biological effects at lower concentrations (10–100 nM) than LPA (250–5000 nM). Using murine fibroblastic NIH3T3 cells and human melanoma A2058 cells, we demonstrate two biological effects that are identical for S1P alone or for SPC + ATX: (*a*) inhibition of ATX- and LPA-stimulated motility; and (*b*) elevation of GTP-Rho signaling above levels induced by ATX alone. PDGF-stimulated motility in NIH3T3 cells was not inhibited by similar concentrations of S1P, indicating that S1P does not cause a general dysregulation of motility and is specific in its inhibitory effects. Finally, using mutant isoforms of ATX deficient in nucleotide hydrolysis, (T210A, H316Q, and H360Q; Ref. 18), we provide evidence that ATX has a common structural requirements for the hydrolysis of SPC and nucleotides.

S1P is known to have a complex relationship to cellular motility (28, 29). S1P stimulates PTX-sensitive motility in endothelial cells (30, 31). In vascular smooth muscle cells, S1P stimulates PTX-sensitive motility at nanomolar concentrations, but at micromolar concentrations it inhibits PDGF-stimulated motility (29, 32). In our tested cell lines, S1P inhibited motility induced by maximally effective concentrations of either ATX or LPA at 10–100 nM concentrations. At 10–25 nM concentrations, S1P had no effect on motility induced by PDGF in 3T3 cells; but at higher concentrations (50–100 nM), it was slightly inhibitory. Other cell lines have been similarly sensitive to S1P inhibition of motility (10–100 nM), including the mouse melanoma cell line B16/F1 stimulated by FCS-containing conditioned medium (33); human neutrophils stimulated by interleukin-8 or f-Met-Leu-Phe (34); and several human breast cancer lines stimulated by fibroblast conditioned medium (35). S1P also appears to have a complex relationship to invasiveness, inhibiting the invasion of B16/F1 melanoma cells through a Matrigel barrier (32), but stimulating invasion of primitive murine hematopoietic cells (THS119) through a stromal barrier (36). Unlike the complexity that characterizes the relationship of S1P to migration and invasion, S1P appears to play a sustained stimulatory and regulatory role in angiogenesis. It stimulates endothelial cell chemotaxis at nanomolar concentration (12, 30, 31, 37), it stimulates the formation of endothelial cell adherens junctions (38), and it regulates endothelial monolayer barrier integrity (39).

Our migration data (Fig. 2 and Fig. 3*D*) indicate that inhibition by S1P is dominant over the migratory response to either exogenous LPA or to the product of an endogenous, natural substrate. The fact that ATX consistently increases motility in multiple cell lines (8) suggests that the major substrate for ATX is a lyso-glycerophospholipid such as LPC (10), which results in production of LPA. However, the exoenzyme ATX has broad substrate specificity, and substrate availability can vary locally. LPA is found in serum in micromolar concentrations, more than half of which is thought to result from the activity of serum lyso-LPD (*i.e.*, ATX) on secreted lyso-glycerophospholipids (10). In contrast, activated platelets are thought to be the major source of serum S1P, produced as a breakdown product of sphingosine by the activity of sphingosine kinase and secreted directly (40). Nonetheless, SPC has been found in rabbit plasma associated with high-density lipoproteins (41) and in the ascites of ovarian cancer patients (42), indicating that SPC is present extracellularly. In addition, SPC has its own specific receptors (43, 44) with a number of functions distinct from S1P (reviewed in Ref. 24). Therefore, the *in vivo* effects of ATX are likely to depend on conditions within the microenvironment, including the concentration of ATX, the availability of SPC *versus* LPC, and the spectrum of Edg receptors expressed by local cells.

The observation that S1P inhibits the stimulation of migration by exogenous LPA argues that S1P acts downstream of LPA production to exert its inhibitory effects, presumably initiated by S1P-specific receptors. Both S1P and LPA are known to activate cells via G protein-coupled Edg receptors. To correlate Edg receptors with observed activities, we examined the Edg receptor expression in A2058 and NIH3T3 clone7 cells. Both cell lines express all three of the LPA receptors (Edg-2/$LPA_1$, Edg-4/$LPA_2$, and Edg-7/$LPA_3$). Edg-4/$LPA_2$ has been associated with LPA-stimulated migration in Jurkat T cells (45), and both Edg-2/$LPA_1$ and Edg-4/$LPA_2$ have been associated with changes in cell shape and actin polymerization (46). However, on the basis of our data we are unable to determine which LPA receptors might be required for an LPA-stimulated migration response. A2058 and NIH3T3 clone7 cells also express two S1P receptors (Edg-5/$S1P_2$ and Edg-3/$S1P_3$). The expression pattern of S1P receptors in the NIH3T3 clone7 cells used in this study differs from that reported for uncloned NIH3T3 cells (47), which express Edg-1/$S1P_1$, as well as Edg-3/$S1P_3$ and Edg-5/$S1P_2$. These two NIH3T3 cell lines are different in their morphology and tumorigenicity (17) as well, but the correlation between these differences and S1P receptor expression is not known. Both Edg-5/$S1P_2$ and Edg-3/$S1P_3$ have been shown to mediate the PTX-insensitive activation of Rho (14), similar to the effect of S1P seen in this present study. Edg-5/$S1P_2$ has been implicated in inhibition of migration (28, 48). In contrast Edg-3/$S1P_3$, along with Edg-1/$S1P_1$, has been associated with a positive migration response to S1P (28). Because our cells failed to migrate to S1P in the presence of Edg-3/$S1P_3$ receptors, it appears that inhibition of migration is the dominant response when both Edg-5/$S1P_2$ and Edg-3/$S1P_3$ are expressed. The hypothesis that S1P exerts its inhibitory effects by engagement of Edg receptors is additionally supported both by the detection of Edg-5/$S1P_2$ and Edg-3/$S1P_3$ proteins on immunoblot (for A2058 cells) and by positive signaling responses (for both tested cell lines). Specifically, we found a positive correlation between high levels of GTP-Rho and the inhibition of migration.

Previous reports of relationships between S1P and PDGF signaling include examples of positive cooperation between Edg-1/$S1P_1$ and PDGF-R (49), as well as inhibition of PDGF signaling (migration) by S1P (29, 32, 48, 50). Our data for NIH3T3 clone7 cells present a third scenario that differs in directionality, *i.e.*, PDGF inhibits S1P signaling.

We have long known that the tumor motility-stimulating protein ATX possesses enzymatic activity, and that this activity is necessary for its stimulation of migration and invasion (4, 23). Previous reports have shown that ATX hydrolyzes lyso-glycerophospholipids to produce LPA, which may mediate many of the documented effects of ATX (8–10). In this article, we present evidence that ATX hydrolyzes the phosphosphingolipid, SPC, into S1P. The physiological effects of these bioactive products of ATX can be homologous or antagonistic. For example, LPA stimulates migration in many different cells; S1P stimulates endothelial cell migration but inhibits motility of many other cells. Depending on cell type both phospholipids can stimulate cell growth, alter cell morphology, affect angiogenesis, or protect against apoptosis (12, 14, 51). Therefore, the exoenzyme ATX might play a complex regulatory role in the cellular microenvironment, potentially either positive or negative, affected by the local availability of substrates and receptors.

## REFERENCES


1. Murata, J., Lee, H. Y., Clair, T., Krutzsch, H. C., Arestad, A. A., Sobel, M. E., Liotta, L. A., and Stracke, M. L. cDNA cloning of the human tumor motility-stimulating protein, autotaxin, reveals a homology with phosphodiesterases. J. Biol. Chem., *269:* 30479–30484, 1994.
2. Goding, J. W., Terkeltaub, R., Maurice, M., Deterre, P., Sali, A., and Belli, S. I. Ecto-phosphodiesterase/pyrophosphatase of lymphocytes and non-lymphoid cells: structure and function of the PC-1 family. Immunol. Rev., *161:* 11–26, 1998.
3. Stefan, C., Gijsbers, R., Stalmans, W., and Bollen, M. Differential regulation of the expression of nucleotide pyrophosphatases/phosphodiesterases in rat liver. Biochim. Biophys. Acta, *1450:* 45–52, 1999.
4. Nam, S. W., Clair, T., Schiffmann, E., Liotta, L. A., and Stracke, M. L. A sensitive screening assay for secreted motility-stimulating factors. Cell Motil. Cytoskelet., *46:* 279–284, 2000.
5. Nam, S. W., Clair, T., Kim, Y. S., McMarlin, A., Schiffmann, E., Liotta, L. A., and Stracke, M. L. Autotaxin (NPP-2), a metastasis-enhancing motogen, is an angiogenic factor. Cancer Res., *61:* 6938–6944, 2001.
6. Bachner, D., Ahrens, M., Betat, N., Schroder, D., and Gross, G. Developmental expression analysis of murine autotaxin (ATX). Mech. Dev., *84:* 121–125, 1999.
7. Fuss, B., Baba, H., Phan, T., Tuohy, V. K., and Macklin, W. B. Phosphodiesterase I, a novel adhesion molecule and/or cytokine involved in oligodendrocyte function. J. Neurosci., *17:* 9095–9103, 1997.
8. Umezu-Goto, M., Kishi, Y., Taira, A., Hama, K., Dohmae, N., Takio, K., Yamori, T., Mills, G. B., Inoue, K., Aoki, J., and Arai, H. Autotaxin has lysophospholipase D activity leading to tumor cell growth and motility by lysophosphatidic acid production. J. Cell Biol., *158:* 227–233, 2002.
9. Tokumura, A., Majima, E., Kariya, Y., Tominaga, K., Kogure, K., Yasuda, K., and Fukuzawa, K. Identification of human plasma lysophospholipase D, a lysophosphatidic acid-producing enzyme, as autotaxin, a multifunctional phosphodiesterase. J. Biol. Chem., *277:* 39436–39442, 2002.
10. Aoki, J., Taira, A., Takanezawa, Y., Kishi, Y., Hama, K., Kishimoto, T., Mizuno, K., Saku, K., Taguchi, R., and Arai, H. Serum lysophosphatidic acid is produced through diverse phospholipase pathways. J. Biol. Chem., *50:* 48737–48744, 2002.
11. Imamura, F., Horai, T., Mukai, M., Shinkai, K., Sawada, M., and Akedo, H. Induction of *in vitro* tumor cell invasion of cellular monolayers by lysophosphatidic acid or phospholipase D. Biochem. Biophys. Res. Commun., *193:* 497–503, 1993.
12. English, D., Kovala, A. T., Welch, Z., Harvey, K. A., Siddiqui, R. A., Brindley, D. N., and Garcia, J. G. Induction of endothelial cell chemotaxis by sphingosine 1-phosphate and stabilization of endothelial monolayer barrier function by lysophosphatidic acid, potential mediators of hematopoietic angiogenesis. J. Hematother. Stem Cell Res., *8:* 627–634, 1999.
13. Hu, Y. L., Tee, M. K., Goetzl, E. J., Auersperg, N., Mills, G. B., Ferrara, N., and Jaffe, R. B. Lysophosphatidic acid induction of vascular endothelial growth factor expression in human ovarian cancer cells. J. Natl. Cancer Inst., *93:* 762–768, 2001.
14. Takuwa, Y. Subtype-specific differential regulation of Rho family G proteins and cell migration by the Edg family sphingosine-1-phosphate receptors. Biochim. Biophys. Acta, *1582:* 112–120, 2002.
15. Todaro, G. J., Fryling, C., and DeLarco, J. E. Transforming growth factors produced by certain human tumor cells: polypeptides that interact with epidermal growth factor receptors. Proc. Natl. Acad. Sci. USA, *77:* 5258–5262, 1980.
16. Clair, T., Lee, H. Y., Liotta, L. A., and Stracke, M. L. Autotaxin is an exoenzyme possessing 5′-nucleotide phosphodiesterase/ATP pyrophosphatase and ATPase activities. J. Biol. Chem., *272:* 996–1001, 1997.
17. Nam, S. W., Clair, T., Campo, C. K., Lee, H. Y., Liotta, L. A., and Stracke, M. L. Autotaxin (ATX), a potent tumor motogen, augments invasive and metastatic potential of ras-transformed cells. Oncogene, *19:* 241–247, 2000.
18. Koh, E., Clair, T., Woodhouse, E. C., Schiffmann, E., Liotta, L. A., and Stracke, M. L. Site-directed mutations in the tumor-associated cytokine, autotaxin, eliminate nucleotide phosphodiesterase, lysophospholipase D and motogenic activities. Cancer Res., *63:* 2042–2045, 2003.
19. Imamura, S., and Horiuti, Y. Enzymatic determination of phospholipase D activity with choline oxidase. J. Biochem. (Tokyo), *83:* 677–680, 1978.
20. Tamaoku, K., Ueno, K., Akiura, K., and Ohkura, Y. New water-soluble hydrogen donors for the enzymatic photometric determination of hydrogen peroxide. Chem. Pharm. Bull., *30:* 2492–2497, 1982.
21. Bligh, E. C., and Dyer, W. F. A rapid method for total lipid extraction and purification. Can. J. Biochem. Physiol., *37:* 911–917, 1959.
22. Aznavoorian, S., Stracke, M. L., Parsons, J., McClanahan, J., and Liotta, L. A. Integrin $\alpha v\beta 3$ mediates chemotactic and haptotactic motility in human melanoma cells through different signaling pathways. J. Biol. Chem., *271:* 3247–3254, 1996.
23. Lee, H. Y., Clair, T., Mulvaney, P. T., Woodhouse, E. C., Aznavoorian, S., Liotta, L. A., and Stracke, M. L. Stimulation of tumor cell motility linked to phosphodiesterase catalytic site of autotaxin. J. Biol. Chem., *271:* 24408–24412, 1996.
24. Meyer zu Heringdorf, D., Himmel, H. M., and Jakobs, K. H. Sphingosylphosphorylcholine–biological functions and mechanisms of action. Biochim. Biophys. Acta, *1582:* 178–189, 2002.
25. Pyne, S., and Pyne, N. J. Sphingosine 1-phosphate signalling in mammalian cells. Biochem. J., *349:* 385–402, 2000.
26. Stracke, M. L., Krutzsch, H. C., Unsworth, E. J., Arestad, A., Cioce, V., Schiffmann, E., and Liotta, L. A. Identification, purification, and partial sequence analysis of autotaxin, a novel motility-stimulating protein. J. Biol. Chem., *267:* 2524–2529, 1992.
27. Hla, T., Lee, M. J., Ancellin, N., Paik, J. H., and Kluk, M. J. Lysophospholipids–receptor revelations. Science (Wash. DC), *294:* 1875–1878, 2001.
28. Okamoto, H., Takuwa, N., Yokomizo, T., Sugimoto, N., Sakurada, S., H., S., and Takuwa, Y. Inhibitory regulation of Rac activation, membrane ruffling, and cell migration by the G protein-coupled sphingosine-1-phosphate receptor EDG5 but not EDG1 or EDG3. Mol. Cell. Biol., *2000:* 9247–9261, 2000.
29. Boguslawski, G., Grogg, J. R., Welch, Z., Ciechanowicz, S., Sliva, D., Kovala, A. T., McGlynn, P., Brindley, D. N., Rhoades, R. A., and English, D. Migration of vascular smooth muscle cells induced by sphingosine 1-phosphate and related lipids: potential role in the angiogenic response. Exp. Cell Res., *274:* 264–274, 2002.
30. Wang, F., Van Brocklyn, J. R., Hobson, J. P., Movafagh, S., Zukowska-Grojec, Z., Milstien, S., and Spiegel, S. Sphingosine 1-phosphate stimulates cell migration through a G(i)-coupled cell surface receptor. Potential involvement in angiogenesis. J. Biol. Chem., *274:* 35343–35350, 1999.
31. Panetti, T. S., Nowlen, J., and Mosher, D. F. Sphingosine-1-phosphate and lysophosphatidic acid stimulate endothelial cell migration. Arterioscler. Thromb. Vasc. Biol., *20:* 1013–1019, 2000.
32. Bornfeldt, K. E., Graves, L. M., Raines, E. W., Igarashi, Y., Wayman, G., Yamamura, S., Yatomi, Y., Sidhu, J. S., Krebs, E. G., Hakomori, S., and *et al.* Sphingosine-1-phosphate inhibits PDGF-induced chemotaxis of human arterial smooth muscle cells: spatial and temporal modulation of PDGF chemotactic signal transduction. J. Cell Biol., *130:* 193–206, 1995.
33. Sadahira, Y., Ruan, F., Hakomori, S., and Igarashi, Y. Sphingosine 1-phosphate, a specific endogenous signaling molecule controlling cell motility and tumor cell invasiveness. Proc. Natl. Acad. Sci. USA, *89:* 9686–9690, 1992.
34. Kawa, S., Kimura, S., Hakomori, S., and Igarashi, Y. Inhibition of chemotactic motility and trans-endothelial migration of human neutrophils by sphingosine 1-phosphate. FEBS Lett., *420:* 196–200, 1997.
35. Wang, F., Van Brocklyn, J. R., Edsall, L., Nava, V. E., and Spiegel, S. Sphingosine-1-phosphate inhibits motility of human breast cancer cells independently of cell surface receptors. Cancer Res., *59:* 6185–6191, 1999.
36. Yanai, N., Matsui, N., Furusawa, T., Okubo, T., and Obinata, M. Sphingosine-1-phosphate and lysophosphatidic acid trigger invasion of primitive hematopoietic cells into stromal cell layers. Blood, *96:* 139–144, 2000.
37. Lee, O. H., Kim, Y. M., Lee, Y. M., Moon, E. J., Lee, D. J., Kim, J. H., Kim, K. W., and Kwon, Y. G. Sphingosine 1-phosphate induces angiogenesis: its angiogenic action and signaling mechanism in human umbilical vein endothelial cells. Biochem. Biophys. Res. Commun., *264:* 743–750, 1999.
38. Lee, M-J., Thangada, S., Claffey, K. P., Ancellin, N., Liu, C. H., Kluk, M., Volpi, M. Sha'afi, R. I., and Hla, T. Vascular endothelial cell adherens junction assembly and morphogenesis induced by sphingosine-1-phosphate. Cell, *99:* 301–312, 1999.
39. Garcia, J. G., Liu, F., Verin, A. D., Birukova, A., Dechert, M. A., Gerthoffer, W. T., Bamberg, J. R., and English, D. Sphingosine 1-phosphate promotes endothelial cell barrier integrity by Edg-dependent cytoskeletal rearrangement. J. Clin. Investig., *108:* 689–701, 2001.
40. Sano, T., Baker, D., Virag, T., Wada, A., Yatomi, Y., Kobayashi, T., Igarashi, Y., and Tigyi, G. Multiple mechanisms linked to platelet activation result in lysophosphatidic acid and sphingosine 1-phosphate generation in blood. J. Biol. Chem., *277:* 21197–21206, 2002.
41. Liliom, K., Sun, G., Bunemann, M., Virag, T., Nusser, N., Baker, D. L., Wang, D. A., Fabian, M. J., Brandts, B., Bender, K., Eickel, A., Malik, K. U., Miller, D. D., Desiderio, D. M., Tigyi, G., and Pott, L. Sphingosylphosphocholine is a naturally occurring lipid mediator in blood plasma: a possible role in regulating cardiac function via sphingolipid receptors. Biochem. J., *355:* 189–197, 2001.
42. Xiao, Y. J., Schwartz, B., Washington, M., Kennedy, A., Webster, K., Belinson, J., and Xu, Y. Electrospray ionization mass spectrometry analysis of lysophospholipids in human ascitic fluids: comparison of the lysophospholipid contents in malignant vs nonmalignant ascitic fluids. Anal. Biochem., *290:* 302–313, 2001.
43. Xu, Y., Zhu, K., Hong, G., Wu, W., Baudhuin, L. M., Xiao, Y., and Damron, D. S. Sphingosylphosphorylcholine is a ligand for ovarian cancer G-protein-coupled receptor 1. Nat. Cell Biol., *2:* 261–267, 2000.
44. Zhu, K., Baudhuin, L. M., Hong, G., Williams, F. S., Cristina, K. L., Kabarowski, J. H., Witte, O. N., and Xu, Y. Sphingosylphosphorylcholine and lysophosphatidylcholine are ligands for the G protein-coupled receptor GPR4. J. Biol. Chem., *276:* 41325–41335, 2001.
45. Zheng, Y., Kong, Y., and Goetzl, E. J. Lysophosphatidic acid receptor-selective effects on Jurkat T cell migration through a Matrigel model basement membrane. J. Immunol., *166:* 2317–2322, 2001.
46. Fukushima, N., Ishii, I., Habara, Y., Allen, C. B., and Chun, J. Dual regulation of actin rearrangement through lysophosphatidic acid receptor in neuroblast cell lines: actin depolymerization by Ca(2+)-$\alpha$-actinin and polymerization by rho. Mol. Biol. Cell., *13:* 2692–2705, 2002.
47. Yamamura, S., Hakomori, S., Wada, A., and Igarashi, Y. Sphingosine-1-phosphate inhibits haptotactic motility by overproduction of focal adhesion sites in B16 melanoma cells through EDG-induced activation of Rho. Ann. N. Y. Acad. Sci., *905:* 301–307, 2000.
48. Ryu, Y., Takuwa, N., Sugimoto, N., Sakurada, S., Usui, S., Okamoto, H., Matsui, O., and Takuwa, Y. Sphingosine-1-phosphate, a platelet-derived lysophospholipid mediator, negatively regulates cellular Rac activity and cell migration in vascular smooth muscle cells. Circ. Res., *90:* 325–332, 2002.
49. Hobson, J. P., Rosenfeldt, H. M., Barak, L. S., Olivera, A., Poulton, S., Caron, M. G., Milstien, S., and Spiegel, S. Role of the sphingosine-1-phosphate receptor EDG-1 in PDGF-induced cell motility. Science (Wash. DC), *291:* 1800–1803, 2001.
50. Osada, M., Yatomi, Y., Ohmori, T., Ikeda, H., and Ozaki, Y. Enhancement of sphingosine 1-phosphate-induced migration of vascular endothelial cells and smooth muscle cells by an EDG-5 antagonist. Biochem. Biophys. Res. Commun., *299:* 483–487, 2002.
51. Tigyi, G. Physiological responses to lysophosphatidic acid and related glycerophospholipids. Prostaglandins, *64:* 47–62, 2001.